35th Annual International Conference of the IEEE EMBS
Osaka, Japan, 3 - 7 July, 2013

Bloch Simulations towards Direct Detection of Oscillating Magnetic Fields using MRI with Spin-lock Sequence*

Shizue Nagahara and Tetsuo Kobayashi, *Member, IEEE*

***Abstract*— A new MRI method using the spin-lock sequence has attracted wide attention because of its potential for detecting small oscillating magnetic fields. However, as the mechanism involved is complicated, we visualized the magnetization performance during the spin-lock sequence in order to better understand interaction of the spin-lock pulse and the externally applied oscillating magnetic fields by means of a fast-and-simple method using matrix operations to solve a time-dependent Bloch equation. To improve spin-lock imaging in the detection of small magnetic fields (in an fMRI experiment that modeled neural magnetic fields), we observed that the phenomenon decreases MR signals, which led us to investigate how spin-lock parameters cause the MR signal to decrease; based on this, we determined that MR signals decrease in oscillating magnetic fields that are resonant with the spin-lock pulse. We also determined that MR signals decrease is directly proportional to spin-lock duration. Our results suggest that MRI can feasibly detect oscillating magnetic fields directly by using of the spin-lock sequence.**

I. Introduction

Functional magnetic resonance imaging (fMRI) is a very powerful tool for the noninvasive detection of neural activities. As the conventional fMRI is based on a blood oxygenation level dependent (BOLD) contrast, in order to visualize the effects of hemodynamic response after brain activation [1], it is limited in terms of temporal and spatial resolution. In recent years, expectations have been raised for the arrival of fMRI methods that can detect neural magnetic fields directly [2]–[5]. Although there have been no reported fMRI experiments in which neural magnetic fields have been successfully detected, some researchers claim that such fields are observable with MRI scanners [2], [5], [6], and have been trying to visualize changes in phase or in magnitude of magnetization generated by subtle and transient alternations of static magnetic fields (B_0) resulting from neural activities. However, this method can be affected by phase cancellation induced by incoherent neuron orientation.

Spin-lock imaging is another reported method for achieving fMRI focusing on neural magnetic fields [7], [8]. As this imaging method—which is based on the spin-lock sequence—does not observe changes in phase or the magnitude of magnetization, but instead visualizes the secondary magnetic resonance between a spin-lock pulse and neural magnetic fields, it has more potential to clearly detect neural magnetic fields. It has a further advantage in that it can potentially detect alternating magnetic fields, such as α (8–13 Hz) and γ waves (25–150 Hz) [9].

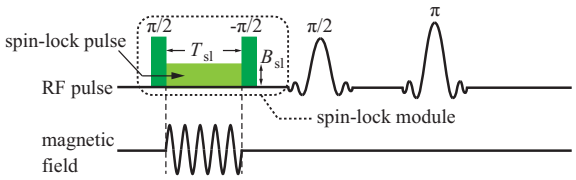

Figure 1. Spin-lock prepared spin echo pulse sequence. As spin-lock module consisting of two π/2 pulses with a spin-lock pulse between them precedes a conventional spin-echo sequence. B_{sl} and T_{sl} are the amplitude and duration time, respectively, of the spin-lock pulse.

To better understand how the spin-lock imaging can detect the magnetic fields, we evaluated the magnetization behavior in the laboratory frame and visualized it, by calculating the Bloch equation by means of a numerical method [10]. We also confirmed that a secondary magnetic resonance occurs when both the spin-lock pulse and the modeled neural magnetic fields satisfy various conditions.

II. Theory

The spin-lock, which is shown in Fig. 1, consists of a spin-lock module containing two π/2 pulses with a spin-lock pulse between them and a conventional spin-echo sequence. The first π/2 pulse and the spin-lock pulse (with amplitude B_{sl} and pulse duration T_{sl}) are applied parallel to the x and y axes, respectively, whereas the second π/2 pulse is applied in the inverse direction to the first one.

The first π/2 pulse flips the initial magnetization, which is aligned along the direction of the static magnetic field B_0 (the z -axis), into the transverse plane (the x-y plane). Then, while the spin-lock pulse is applied along the y -axis, this flipped magnetization is locked into the transverse plane by the spin-lock field B_{sl}. In the frame rotating with the resonance frequency of B_0, B_{sl} acts as a secondary B_0 field; therefore, a magnetic field oscillating at a resonance frequency of B_{sl} ($\omega_{sl} = \gamma B_{sl}$), flips the magnetization direction. After time T_{sl}, the second π/2 pulse is applied and restores the magnetization y along the z -axis. By renaming the axes x to y, y to z, and z to x in the doubly rotating frame, the Bloch equation for magnetization $\mathbf{M} = (M_x, M_y,$

*This work was partially supported by a Grant-in-Aid for Challenging Exploration Research (24650221) , a Graint-in-Aid for Scientific Research (A) (24240081) and a Grant-in-Aid for JSPS Fellows (No. 023·5348) all from the Ministry of Education, Culture, Sports, Science and Technology (MEXT), Japan.

S. Nagahara is with Department of Electrical Engineering, Graduate School of Engineering, Kyoto University, Kyotodaigaku-katsura, Nishikyo-ku, Kyoto-shi, Kyoto, 615–8510, Japan and a research fellow of the Japan Society for the Promotion of Science (corresponding author to provide phone: 075-383-2233; fax: 075-383-2259; e-mail: nagahara@bfe.kuee.kyoto-u.ac.jp)

T. Kobayashi is with Department of Electrical Engineering, Graduate School of Engineering, Kyoto University, Kyotodaigaku-katsura, Nishikyo-ku, Kyoto-shi, Kyoto, 615–8510, Japan (e-mail: tetsuo@kuee.kyoto-u.ac.jp)

978-1-4577-0216-7/13/$26.00 ©2013 IEEE

M_z) behavior during the spin-lock pulse can be formulated:

$$\begin{aligned} \frac{dM_x}{dt} &= -\frac{M_x}{T_2^*} + (\omega_{\rm sl} - \omega)M_y \\ \frac{dM_y}{dt} &= -(\omega_{\rm sl} - \omega)M_x - \frac{M_y}{T_2^*} + \omega_{\rm m}M_z \\ \frac{dM_z}{dt} &= -\omega_{\rm m}M_y - \frac{M_z - M_0}{T_{1\rho}} \end{aligned} \quad (1)$$

where, $\omega_{\rm m}$ = $\gamma B_{\rm m}$. $B_{\rm m}$ and ω are the amplitude and frequency of the oscillating magnetic field, respectively, and $T_{1\rho}$ and T_2^* represent the $T_{1\rho}$ and T_2^* relaxation time, respectively. Following application of the spin-lock module, a spin-echo imaging sequence generates MR signals.

While using this spin-echo sequence with spin-lock module, an externally applied oscillating magnetic field decrease the MR signal owing to a secondary magnetic resonance with the spin-lock field. Based on this effect, by focusing on neural magnetic fields oscillating at specific frequencies— such as α and γ waves— it is possible to conduct fMRI studies with the spin-lock sequence [7], [8].

III. Methods

First, the magnetization behavior in the doubly rotating frame during the spin-lock pulse was calculated by means of a matrix operation [10]. The three components of magnetization shown in Eq. 1 were transformed in to a singly rotating frame and assosiated with the magnetization behavior during the π/2 pulses. Finally, the singly rotating frame components were transformed into the laboratory frame to derive the time-dependent magnetization behavior.

In order to observe the secondary magnetic resonance of the spin-lock and the neural magnetic fields via Bloch simulation, we obtained the signal intensities with a spin-lock pulse at fixed amplitudes of $B_{\rm sl}$ of 0.235, 1.17, and 2.35 μT while changing the frequency ω of the oscillating magnetic field. The Larmor frequencies corresponding to these fixed amplitudes were 10, 50, and 100 Hz, respectively, and T_1, T_2^* and $T_{1\rho}$ were set to 1100, 75 and 100 ms, respectively, in order to model human brain gray matter scanned with 1.5 Tesla MRI [11], [12]. To obtain $\omega_{\rm m}$, $B_{\rm m}$ was fluctuated between 0.5, 1.0, and 5.0 nT while T_{sl} was fixed at 100 ms.

Bloch simulations was also used to investigate another parameter of spin-lock pulse— the influence of $T_{\rm sl}$ on signal decrease during secondary magnetic resonance. At the same value of T_1, T_2^*, and $T_{1\rho}$, we increased $T_{\rm sl}$ from 0 to 500 ms while changing $B_{\rm m}$ to 0.5, 1.0 and 5 nT. To simulate the secondary magnetic resonance $B_{\rm sl}$ and ω were set to 2.35 μT ($\omega_{\rm sl}$ = 100 Hz) and 100 Hz, respectively.

IV. Results

Figs. 2(a) and 2(b) show the magnetization behaviors during application of the spin-lock module without and with an externally applied oscillating magnetic field. Magnetization [$M_{\rm x}$, $M_{\rm y}$, $M_{\rm z}$] commenced at [0, 0, 1] and was then flipped into the x-y plane as shown Fig. 2(a). After locked in x-y plane, the magnetization returned to the z -axis. The decrease in final $M_{\rm z}$ is caused solely by $T_{1\rho}$ relaxation. In contrast, the magnetization that started under the conditions shown in Fig. 2(a) oscillated three-dimensionally, as shown in Fig. 2(b), as the magnetic field oscillating at the Larmor frequency of the spin-lock pulse flipped it into the plane perpendicular to the spin-lock direction acting like π/2 excitation pulse.

Fig. 3 shows that the ratio $M_{\rm z}$ (on) / $M_{\rm z}$ (off) decreased when the applied magnetic field was oscillating at a Larmor frequency of $\gamma B_{\rm sl}$, as can be seen from the secondary magnetic resonances with $B_{\rm m}$ at 0.5 and 1.0 nT in Fig. 3 (a) and with $B_{\rm m}$ at 5.0 nT in Fig. 3 (b). It is obvious from these figures that larger values of $B_{\rm m}$ correspond to larger decreases in $M_{\rm z}$ (on) / $M_{\rm z}$ (off); this can be explained as an effect of the increase in the amplitude of rotation of $M_{\rm z}$ with increasing $B_{\rm m}$.

We also investigated the influence of $T_{\rm sl}$ on the decrease in magnetization during the secondary magnetic resonance. Fig. 4 shows the magnetization decrease ($M_{\rm z}$ (off) - $M_{\rm z}$ (on)) / $M_{\rm z}$ (off)) as a function of $T_{\rm sl}$ on a semi-logarithmic plot for three values of $B_{\rm m}$. The results of this assessment show that the magnetization decrease is larger at larger values of $T_{\rm sl}$ as the magnetization is rotated in proportion to the duration of $T_{\rm sl}$. As shown in Fig. 3, we also obtained similar results for the influences of $B_{\rm m}$, which also originate from the amplitude of rotation in $M_{\rm z}$.

V. Discussion

Several previous studies tried to detect neural magnetic fields using MRI, cell cultures, and theoretical calculations [2], [3], [13], [14]. Most of these approached the problem by trying to observe changes in magnitude or phase images; however, this strategy has the disadvantage of cancellation effects owing to spatially disordered structures, oscillation with a mean phase change of zero, incoherent signals, and the location of the current source within the given image voxel [8], [13].

In contrast to this approach, spin-lock imaging can potentially detect such signals without cancellations in the magnitude or phase images; it can provide $T_{1\rho}$-weighted images, as has been previously done in biomedical imaging [15], and has advantage of allowing band-selective variants of the experiments such as those shown in Fig. (3). As such, spin-lock imaging would be of great use in measuring biological sources with multiple consistent frequencies [8].

To use spin-lock imaging for fMRI, it must be sufficiently sensitive to neural magnetic fields. Although the possibility of detecting such fields is still matter of debate, some research groups have already reported that they could measure the magnetic fields of sub-nT order using different methods [2], [3], [7], [8]. Magnetoencephalography (MEG) measurements suggest that evoked or spontaneously synchronized synaptic activity in the 50,000 or more cortical neurons occupying an area of one or a few mm^2 results in magnetic fields on the order of 0.1 – 1 pT at a distance of 2$\sim$4 cm away from the neuronal source. By contrast, MRI focusing on voxels at 2$\sim$4 mm away from the site of activation, equates to fields on the order of 0.1 – 1 nT (based on an inverse-square

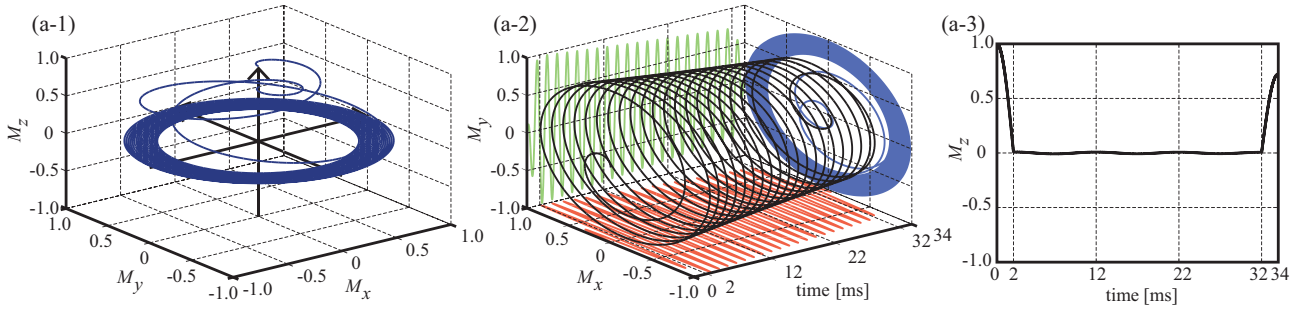

(a) Magnetization behavior without oscillating magnetic field

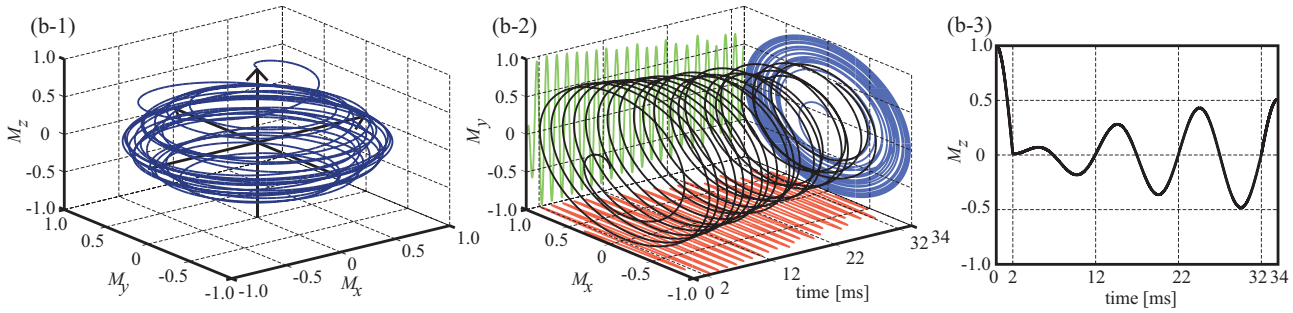

(b) Magnetization behavior with oscillating magnetic field

Figure 2. The magnetization behavior during spin-lock module without oscillating magnetic field applied (a-1). The time courses of x and y components of the magnetization (a-2). The time course of z component of the magnetization. The first 2 ms π/2 pulse flipped M_z down to the x-y plane and the second 2 ms π /2 pulse flipped up it to z axis. During the spin-lock pulse, it stayed in x-y plane and was affected by the $T_{1\rho}$ (a-3). The magnetization behavior during spin-lock module with oscillating magnetic field applied (b-1). The time course of x and y components of the magnetization (b-2). The time course of z component of the magnetization. The first 2 ms π/2 pulse flipped M_z down to the x-y plane and the second 2 ms π /2 pulse flipped up it to z axis. During the spin-lock pulse, it oscillated along z axis due to the oscillating magnetic field and was also affected by the $T_{1\rho}$ (b-3). Here, we used the parameters: T_1 = 1100 ms, T_2^* = 75 ms, $T_{1\rho}$ = 100 ms, B_{sl} 2.35 μT (ω_{sl} = 100 Hz), T_{sl} = 30 ms, B_{m} = 0 (a) / 100 (b) ms and ω = 0 (a) / 100 (b) Hz. In addition, we chose B_0 = 1.5 $\times$ 10^{-5} T to visualize the magnetization behavior clearly.

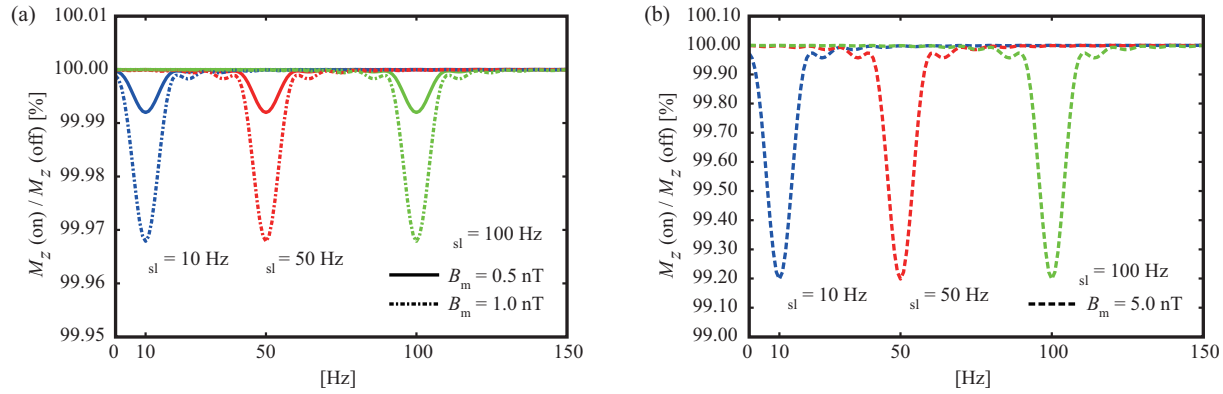

Figure 3. Percent signal changes originating from secondary magnetic resonance. M_z (on) and M_z (off) indicate z component of the magnetization at the end of spin-lock module with and without oscillating magnetic field, respectively. The normalized magnetization (M_z (on) / M_z (off)) decreases while ω_{sl} and ω are on resonance: 10 Hz, 50 Hz and 100 Hz: B_{m} = 0.5 and 1.0 nT (a), B_{m} = 5.0 nT (b). As the conventional spin echo sequence starts right after the spin-lock module, the decreased normalized magnetization leads to the decrease of MR signals.

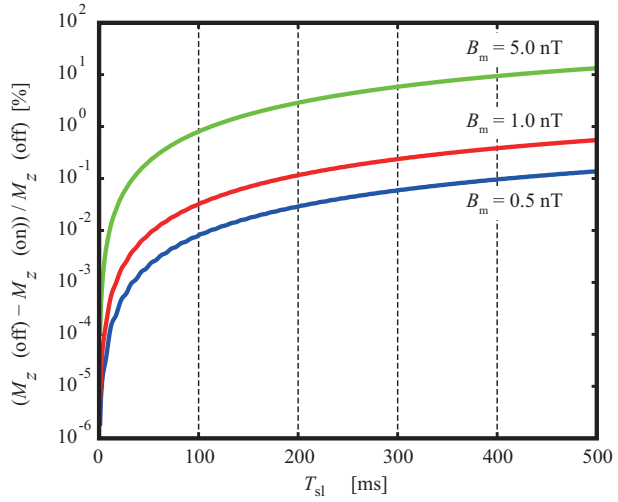

Figure 4. Percent signal decrease on the condition of secondary magnetic resonance. M_z (on) and M_z (off) indicate z component of the magnetization at the and of spin-lock module with and without oscillating magnetic field, respectively. The T_{sl} dependencies were simulated with the B_{sl} of 0.5, 1.0 and 5.0 nT.

distance scale $(r_{\mathrm{MEG}} \ / \ r_{\mathrm{MRI}})^2)$) [3]. Moreover, research estimating neural magnetic fields using model calculation has claimed that 1,000,000 randomly oriented dipoles (i.e., dendrites) within 1 mm^3 generate a magnetic field of 0.22 nT [5].

It is thus essential to be able to detect magnetic fields of 0.1 – 1 nT in order to measure brain activation with MRI. However, it can be seen from Fig. (3) that M_z decreases by only 0.008 and 0.032 % owing to the effects of oscillating magnetic fields of 0.5 and 1.0 nT, respectively. Even a 5 nT field can cause a 0.80 % decrease in M_z, which is much smaller than BOLD signal changes. This implies that for the fMRI experiments an improvement of signal to noise ratio is necessary; i.e., increasing the number of measurement repetition. Employing a longer $\mathrm{T_{sl}}$ is another way to increase the signal changes (from Fig. 4 it can be seen that a longer $\mathrm{T_{sl}}$ produces a larger signal decreases). Because it approximately zeros out BOLD and susceptibility artifacts [16], [17], ultra – low field MRI has been attracting attentions as a way to avoid BOLD contamination problems.

Although it does not appear in the Bloch equation(Eq. 1), B_{sl} is another parameter of spin-lock pulse that B_{sl} affects $T_{1\rho}$ [11], [15]. As with T_1 and T_2^*, $T_{1\rho}$ also depends on the magnitude of the static magnetic field B_0, the properties of tissues and the amplitude of the applied spin-lock pulse (this phenomenon is called $T_{1\rho}$ dispersion) [15]. As a result, measurements of $T_{1\rho}$ based on specific imaging conditions will be required in simulation.

In this paper, we demonstrated that our Bloch simulation method is useful in helping to understand the magnetization behavior during application of a spin-lock module. The secondary magnetic resonance that occurs between the spin-lock pulse and externally applied oscillating magnetic fields obviously decreases the value of M_z following spin-lock leading to MR signal reduction. Although our results show that percentage signal changes resulting from spin-lock interactions are much smaller than BOLD effects, we suggest that spin-lock imaging has the potential to allow observation of neural activation directly by increasing the number of repetitions and employing ultra-low field MRIs.

Acknowledgment

The authors thank Dr. Ito, Mr. Ueno, Dr. Imai and Dr. Takayama for their assistance and discussion.

References

[1] S. Ogawa, T. Lee, A. Kay, and D. Tank, "Brain magnetic resonance imaging with contrast dependent on blood oxygenation," *Proceedings of the National Academy of Sciences*, vol. 87, no. 24, pp. 9868–9872, 1990.

[2] J. Bodurka and P. Bandettini, "Toward direct mapping of neuronal activity: Mri detection of ultraweak, transient magnetic field changes," *Magnetic resonance in medicine*, vol. 47, no. 6, pp. 1052–1058, 2002.

[3] N. Petridou, D. Plenz, A. Silva, M. Loew, J. Bodurka, and P. Bandettini, "Direct magnetic resonance detection of neuronal electrical activity," *Proceedings of the National Academy of Sciences*, vol. 103, no. 43, pp. 16 015–16 020, 2006.

[4] N. Höfner, H. Albrecht, A. Cassará, G. Curio, S. Hartwig, J. Haueisen, I. Hilschenz, R. Körber, S. Martens, H. Scheer, *et al.*, "Are brain currents detectable by means of low-field nmr? a phantom study," *Magnetic Resonance Imaging*, vol. 29, no. 10, pp. 1365–1373, 2011.

[5] W. Jay, R. Wijesinghe, B. Dolasinski, and B. Roth, "Is it possible to detect dendrite currents using presently available magnetic resonance imaging techniques?" *Medical and Biological Engineering and Computing*, pp. 1–7, 2012.

[6] T. Park and S. Lee, "Effects of neuronal magnetic fields on mri: numerical analysis with axon and dendrite models," *Neuroimage*, vol. 35, no. 2, pp. 531–538, 2007.

[7] T. Witzel, F. Lin, B. Rosen, and L. Wald, "Stimulus-induced rotary saturation (sirs): A potential method for the detection of neuronal currents with mri," *Neuroimage*, vol. 42, no. 4, p. 1357, 2008.

[8] N. Halpern-Manners, V. Bajaj, T. Teisseyre, and A. Pines, "Magnetic resonance imaging of oscillating electrical currents," *Proceedings of the National Academy of Sciences*, vol. 107, no. 19, pp. 8519–8524, 2010.

[9] R. Canolty, E. Edwards, S. Dalal, M. Soltani, S. Nagarajan, H. Kirsch, M. Berger, N. Barbaro, and R. Knight, "High gamma power is phase-locked to theta oscillations in human neocortex," *science*, vol. 313, no. 5793, pp. 1626–1628, 2006.

[10] K. Murase and N. Tanki, "Numerical solutions to the time-dependent bloch equations revisited," *Magnetic Resonance Imaging*, vol. 29, no. 1, pp. 126–131, 2011.

[11] A. Borthakur, A. Wheaton, A. Gougoutas, S. Akella, R. Regatte, S. Charagundla, and R. Reddy, "In vivo measurement of t1ρ dispersion in the human brain at 1.5 tesla," *Journal of Magnetic Resonance Imaging*, vol. 19, no. 4, pp. 403–409, 2004.

[12] W. Rooney, G. Johnson, X. Li, E. Cohen, S. Kim, K. Ugurbil, and C. Springer, "Magnetic field and tissue dependencies of human brain longitudinal 1h2o relaxation in vivo," *Magnetic Resonance in Medicine*, vol. 57, no. 2, pp. 308–318, 2007.

[13] D. Konn, P. Gowland, and R. Bowtell, "Mri detection of weak magnetic fields due to an extended current dipole in a conducting sphere: a model for direct detection of neuronal currents in the brain," *Magnetic resonance in medicine*, vol. 50, no. 1, pp. 40–49, 2003.

[14] A. Cassara, G. Hagberg, M. Bianciardi, M. Migliore, B. Maraviglia, *et al.*, "Realistic simulations of neuronal activity: a contribution to the debate on direct detection of neuronal currents by mri," *NeuroImage*, vol. 39, no. 1, pp. 87–106, 2008.

[15] S. Charagundla, "T1rho-weighted magnetic resonance imaging: Principles and diagnostic application," *APPLIED RADIOLOGY*, vol. 33, no. 1; SUPP, pp. 32–43, 2003.

[16] R. Kraus Jr, P. Volegov, A. Matlachov, and M. Espy, "Toward direct neural current imaging by resonant mechanisms at ultra-low field," *NeuroImage*, vol. 39, no. 1, pp. 310–317, 2008.

[17] A. Cassará, B. Maraviglia, S. Hartwig, L. Trahms, and M. Burghoff, "Neuronal current detection with low-field magnetic resonance: simulations and methods," *Magnetic resonance imaging*, vol. 27, no. 8, pp. 1131–1139, 2009.